Available online at www.jourcc.com

Journal homepage: www.JOURCC.com

Journal of Composites and Compounds

Development of hybrid electrodeposition/slurry diffusion aluminide coatings on Ni-based superalloy with enhanced hot corrosion resistance

Ali Zakeri [a]* , *Mohammadreza Masoumi Balashadehi* [a], *Alireza Sabour Rouh Aghdam* [a]

[a] *Department of Materials Engineering, Tarbiat Modares University, Tehran P.O. Box: 14115-143, Tehran, Iran*

A B S T R A C T

Ni/Co-modified aluminide coatings were prepared on the Hastelloy-X superalloy by a combined process of electrodeposition and slurry aluminizing. In this regard, pure layers of Ni and Ni-50wt.%Co were initially applied via electrodeposition process and successive aluminization was carried out by a slurry technique. The scanning electron microscopy (SEM) and X-ray diffraction (XRD) techniques were used for the microstructural and chemical composition characterization of the specimens. The results of these analyses revealed that a compact and dense aluminide coating was formed with a two-layered structure containing the outer Al-rich β phase and inner interdiffusion zone. Moreover, the presence of pre-electrodeposited layers inhibited the outward diffusion flux of elements from the substrate and effectively suppressed the formation of Kirkendall pores. The hot corrosion studies of the obtained coatings indicated that the addition of a pre-electrodeposited layer could enhance the high-temperature corrosion performance of the coatings when exposed to sulfate salt.

Peer review under responsibility of JCC Research Group

A R T I C L E I N F O R M A T I O N

Article history:
Received 03 December 2020
Received in revised form 17 January 2021
Accepted 20 March 2021

Keywords:
Diffusion
Electrodeposition
Slurry
Aluminide
Hot corrosion

1. Introduction

Nickel-based superalloys have found extensive applications in gas turbine industries due to their excellent thermo-mechanical properties [1–4]. Oftentimes, these materials are employed in the manufacturing of turbine blades to combat the failure arising from the mechanical aspect, which is provided by increasing the content of refractory elements, such as W, Mo, and Re for creep strength improvement [1]. This, in turn, results in lower environmental degradation resistance due to the reduction in Al content (normally < 7 wt.%), which is critical for the formation of a protective oxide scale [5,6]. In this regard, the surfaces of these materials are typically protected by two types of coatings, namely overlay and diffusion coatings [7 16]. The former coatings are often applied by thermal spray methods which require sophisticated equipment and the operation cost is high. On the other hand, the diffusion coatings can be obtained by simple and cost-effective processes such as pack cementation and slurry aluminizing [17].

Application of the diffusion coatings for airfoils was first employed by using the pack cementation technique in the late 1960s [18]. This process is still considered the most widely used method for applying diffusion coatings and the formation mechanism of coating is well-studied [19,20]. Generally, the protection mechanism provided by the diffusion coatings relies on the enrichment of protective alloying elements at the surface of substrate, which leads to the formation of a uniform oxide scale during exposure to harsh conditions at high temperatures. For this purpose, the enrichment of surface layer with silicon (siliconizing), chromium (chromizing), and aluminum (aluminizing) elements were carried out. It should be mentioned that for applications at temperatures of higher than about 1000 ℃, the most crucial element is Al [21].

Currently, slurry aluminizing has received considerable attention as an alternative method [22,23]. This is because of the advantages in the processing compared to the conventional pack cementation. In addition, among the above mentioned processes, only the slurry aluminizing is capable of providing coatings for the interior surfaces (cooling passage) of the turbine blades [17]. In recent years, there are ongoing studies that are focused on the improvement of high-temperature corrosion behavior of the simple aluminide coatings by the addition of beneficial elements like Zr, Hf, Pt, and Co [24–28]. Chemical modification of the aluminide coatings is considered to be one of the efficient methods in improving the microstructural and oxidation/corrosion properties. A simple and effective strategy to fabricate the modified aluminide coatings is by incorporating an electrodeposited intermediate layer [29–32]. Karimzadeh and Sabour Rouhaghdam [33] investigated the influence of pre-plated Ni layer on the oxidation performance of aluminide coatings. They have pointed out that the presence of a primary electroplated Ni layer could inhibit the formation of Kirkendall pores during aluminizing, as well as improving its oxidation resistance. Furthermore, Safari et al. [34] have reported that the chemical modification of the aluminide coating through electrodeposition of Ni-CeO_2 layer could improve the cyclic oxidation resistance of the obtained coating. In another study by Qiao and Zhou [35], it has been shown that the addition of Co into the simple NiAl coating could lower the oxidation kinetics which was attributed to the formation of a thin and compact film of a-Al_2O_3 onto the coating sur-

* *Corresponding author: Ali Zakeri; E-mail: alizakeri@modares.ac.ir*
DOR: 20.1001.1.26765837.2021.3.6.1.4
https://doi.org/10.52547/jcc.3.1.1

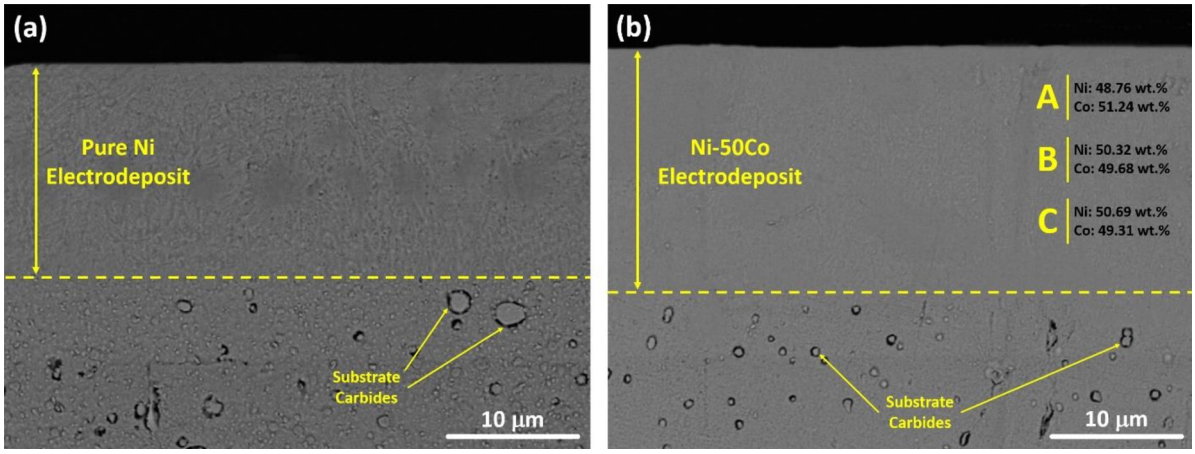

Fig. 1. Cross section of the (a) pure Ni and (b) Ni-50Co electrodeposited layers (the dashed line indicates the interface).

Table 1.
Chemical composition (wt. %) of Hastelloy® X

Element	Ni	Co	Cr	Fe	Mo	W	Al	C	Mn	Si	B
OES Values	Bal.	1.26	20.8	19.67	8.1	0.34	0.21	0.07	0.51	0.22	0.002

face. In a subsequent study conducted by the same authors, it has been found out that the Co-modified NiAl coating exhibited superior hot corrosion resistance and it was ascribed to the formation of a-Al_2O_3 scale promoted by the presence of cobalt [36]. The objective and novelty of this study are to propose a new and efficient approach to the fabrication of Ni/Co-modified aluminide coatings through a combined process of electrodeposition and slurry aluminizing. In addition, the hot corrosion performance of coatings is evaluated and discussed.

2. Materials and methods

2.1. Starting materials and sample preparation

A nickel-based superalloy Hastelloy® X was selected as the substrate material and its chemical composition, determined by the optical emission spectroscopy (OES), are given in Table 1. Several sets of coupons (15 x 5 x 2 mm^3) were cut by electro-discharge machining.

2.2. Electrodeposition process

At the first stage of experimental procedure, the coupons were prepared for electrodeposition by polishing to 600 grit SiC paper, degreasing by acetone and electrochemically activating by anodic oxidation at current density of 10.75 $A.dm^{-2}$ within H_2SO_4 solution for 60 seconds. A typical Watts-type bath, containing nickel sulfate ($NiSO_4.6H_2O$, 200 g/l), nickel chloride ($NiCl_2.6H_2O$, 35 g/l), cobalt sulfate ($CoSO_4.7H_2O$, 0-50 g/l), boric acid (H_3BO_3, 30 g/l), and sodium dodecyl sulfate as surfactant (SDS, 0.6 g/l) was used as the electrodeposition electrolyte. The operating conditions such as current density and temperature were adjusted as 5 $A.dm^{-2}$ and 50 ℃, respectively. Moreover, the pH of the electrolyte was kept constant at 4.0 and two pure Ni plates were used as anode. Afterward, two specimens with pure Ni and Ni-50Co pre-electrodeposited layers were produced.

2.3. Slurry aluminizing process

Initially, the samples were activated by immersion in an acidic solution comprised of 50 ml H_2SO_4, 75 ml HNO_3, 33 ml distilled water, and 1 g NaCl. Then, they were sprayed by a slurry containing spherical aluminum powder as the diffusion coating element source dispersed in a water/ polyvinyl alcohol (PVA) (10:1) mixture. The application of slurry layer was mass-controlled and adjusted in the range of 15-20 mg/cm^2. It should be noted that the application of slurry layer above this range would result in the spallation of slurry layer due to the thermal stresses generated during heating. Prior to placing the samples, the furnace chamber was circulated with argon for three times to eliminate oxygen. Subsequently, the coupons were placed in an alumina crucible and then heated to the processing temperature of 750 and 1050 ℃ for 2 and 1 h, respectively, followed by furnace cooling. An electric tube furnace operating at a heating rate of 10 ℃/min in an Ar atmosphere was used for slurry aluminizing process.

2.4. Hot corrosion test

A muffle furnace with an accuracy of ± 5 ℃ was used to perform the hot corrosion experiments in static air at 900 ℃. Prior to the experiment, all faces of the specimens were hand-brushed with a Na_2SO_4 saturated aqueous salt solution at about 1-2 mg/cm^2 and followed by hot airflow drying. In order to precisely control the mass/area ratio of the applied salt, the samples were weighed before and after supplying the salt. The salt composition used in this study is a typical approach to simulate the environment of materials exposed to regions with high levels of pollutants and it has been previously used by many researchers [37–40]. The samples were subjected to the hot corrosion test for 100 h and were withdrawn from the furnace after the cooling stage. In this study, the corrosion performance was evaluated by comparing the thickness of formed corrosion layer on the coatings' surface, which were measured by using ImageJ software [41]. This method does not involve the common errors associated with the mass change records due to the remaining salt deposits and formation of volatile compounds during the test [42].

2.5. Characterization techniques

The morphological assessment of the specimens was carried out by scanning electron microscopy (SEM, Zeiss, model Evo15) coupled with an X-ray energy dispersive (EDS) analyzer. The microstructure and chemical composition of the hot-corroded samples were also examined by SEM-EDS. In this regard, first the remaining salt was removed by washing the samples in boiling distilled water, then, one of the tested samples was warm-mounted in a plastic resin, ground with SiC abrasive papers (400-3000 grit) and polished to a mirror finish to reveal the cross-section microstructure of the coating and corrosion products layer. The phase analysis was performed by X-ray diffraction (XRD, Philips

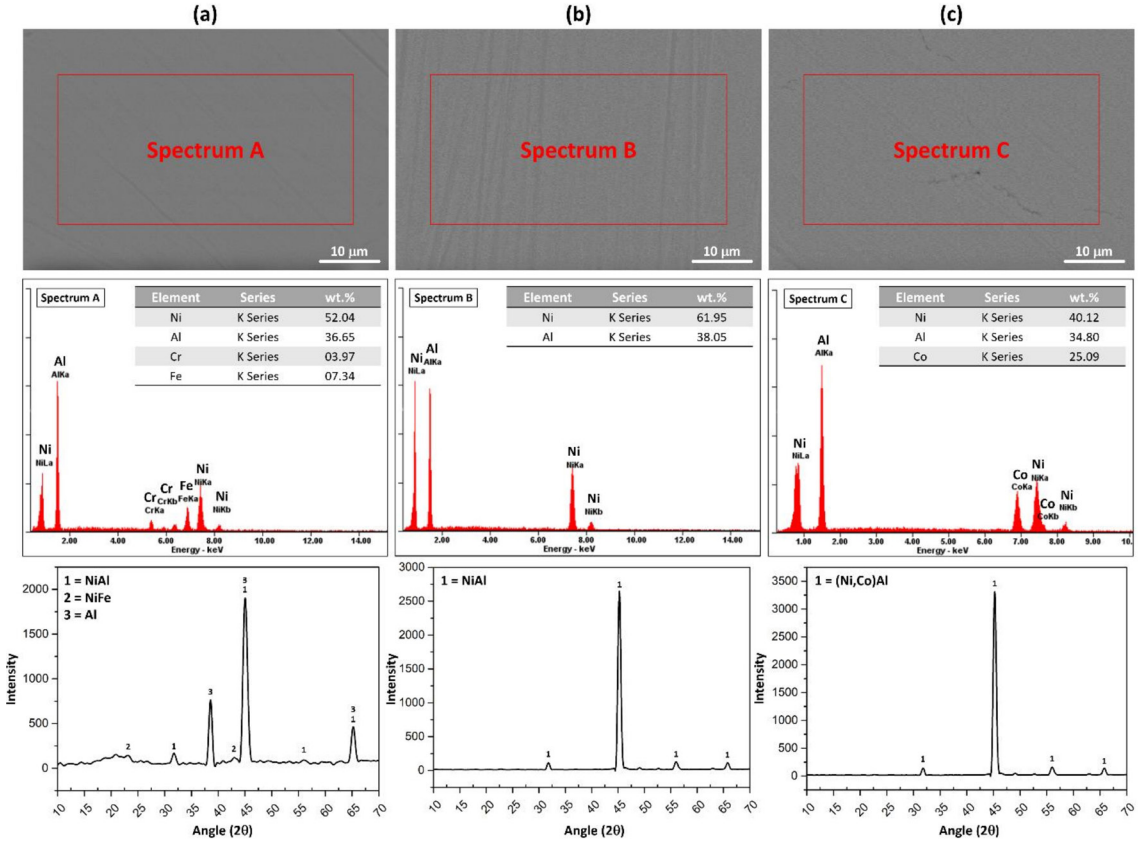

Fig. 2. Surface characteristics of the diffusion coatings; (a) simple, (b) Ni-modified, and (c) Ni/Co-modified aluminide coating.

PW1730, CuKα radiation) and the identification of XRD patterns was made on the basis of the ICDD database [43].

3. Results and discussion

3.1. As-electrodeposited samples

Among the surface engineering techniques, electrodeposition is a common and well-known method owing to its flexibility, moderate costs, and simple procedure [44–47]. Fig. 1 displays the cross-section of the electrodeposited coatings on the superalloy substrates. The average thickness of the mono-layer electrodeposited coatings was within the range of 15-18 mm. It can be noticed from the EDS analysis results that the chemical composition was homogeneous throughout the entire layer and was almost identical in upper, middle, and lower regions. The uniform structure of Ni-Co electrodeposits have been reported in other studies as well [48–50]. Although the samples were etched, no distinct interface between the substrate and the electrodeposited layer was evident from the SEM images. This is because of the nearly identical compositions of the two regions.

3.2. As-aluminized samples

The specimens were followed by slurry aluminizing. Fig. 2 shows the surface morphology images and the corresponding chemical compositions and crystalline structures determined by EDS and XRD analyses, respectively. According to the EDS analyses, it was revealed that only the modified samples showed the main elements of the β-(Ni,Co)Al intermetallic phase. This could be due to the presence of pre-electrodeposited layer onto the surface of the Hastelloy X, where only outward diffusion of Ni and Co occurred. On the other hand, concerning the simple aluminide coating, small amounts of Fe and Cr were detected. These observations may suggest that the electrodeposited layer hinders the outward diffusion from the substrate during slurry aluminizing process [33]. Moreover, the formation of β-phase was confirmed for all of the specimens by the XRD results. That being said, additional NiFe phase was detected for the simple aluminide coating, which may be the consequence of outward Fe diffusion. In addition, strong peaks of metallic Al were detected, which can be the result of un-reacted liquid Al in the slurry.

The formation of slurry diffusion coatings can be explained by the Ni-Al combustion synthesis process [18]. During this process, the melting of Al component is the initiating step. Afterward, through wetting of Ni by Al melt, it dissolves Ni from the surface and the Ni-Al reaction proceeds in the molten state. Based on the Ni concertation in the Al melt, which is dependent on the temperature of the process, one or more phases of $NiAl_3$, Ni_2Al_3, and NiAl can be formed. Taking into account that the processing temperatures used in this study were high and the maximum solubility of Ni in molten Al increases with temperature, the formation of NiAl as the thermodynamically stable phase was anticipated. This was true for the modified coatings, since at the initial stage, the liquid Al came in contact with the pure pre-electrodeposited layers instead of superalloy substrate. It has been reported that pure Ni substrates result in the higher exothermic reactions, which makes it easier for Al to react and form the intermetallic phases [18].

The cross-section SEM-EDS mapping and EDS line scan analyses of the aluminized samples are depicted in Fig. 3 and Fig. 4, respectively. All of the specimens exhibited the formation of a distinct outer NiAl layer with an interdiffusion zone (IDZ), which is a typical microstructure of the aluminide diffusion coatings [33]. This structure, in turn, provides the excellent adhesion of these coatings due to the metallurgical bonding with the substrate [17]. Moreover, the diffusion layer obtained by the slurry process was compact with no evident cracks or segmented parts. The EDS line scan analyses illustrate that the concentration of

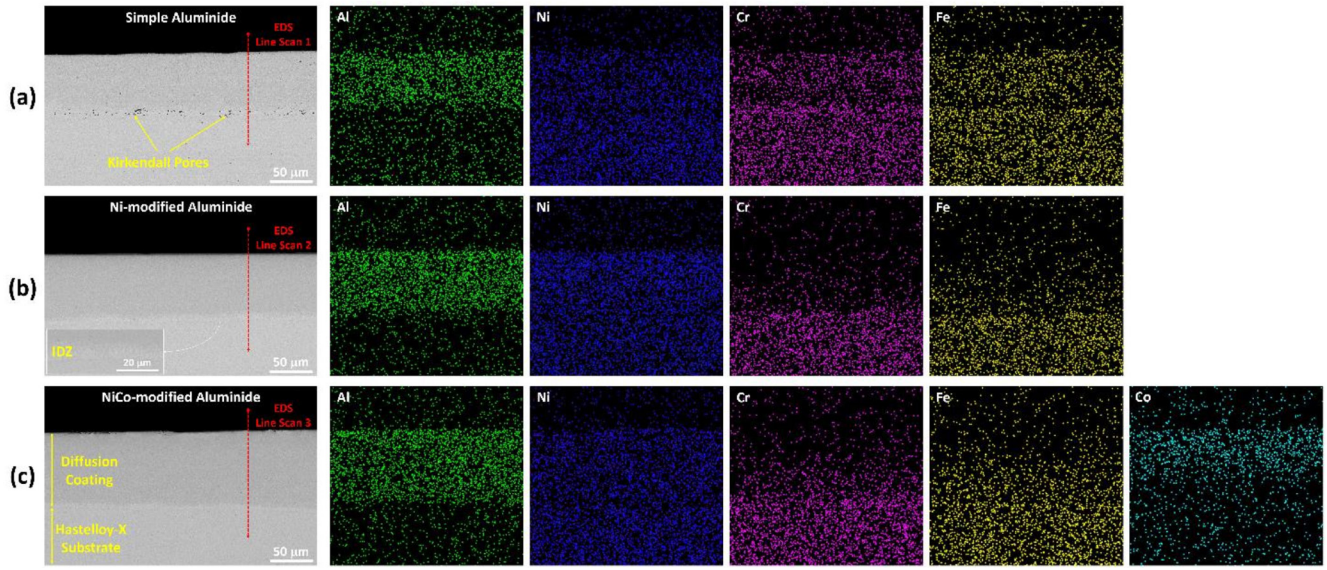

Fig. 3. Cross-section SEM-EDS mapping analyses of the coated samples; (a) simple, (b) Ni-modified, and (c) Ni/Co-modified aluminide coating.

Al was decreased from top surface toward the depth of the superalloy, which contains less Al content. The Al-rich zone indicates the formed aluminide coating and the average thickness was 68±2.71, 75±1.10, and 85±1.59 mm in the case of simple, Ni-modified, and Ni/Co-modified aluminide coatings. As previously mentioned, the presence of pure pre-electrodeposited layers makes the exothermic reactions easier in a Ni-Al diffusion couple, which may result in the increased thickness of the aluminide coating. Moreover, given the fine-grained microstructure of the electrodeposited layers in comparison with the pure substrate, the aluminizing kinetics could be enhanced for the samples with pre-electrodeposited layers, resulting in faster atomic diffusion and larger coating thickness [30].

The main microstructural differences between the simple and modified aluminide coatings can be attributed to the presence of Kirkendall pores and the outward diffusion of substrate elements (Cr and Fe). These phenomena have been reported in other cases of the diffusion aluminide coatings and are mainly related to the microstructural inhomogeneities in the substrate [33]. According to the EDS mapping analyses of the modified coatings, the pre-electrodeposited layers have effectively inhibited the outward diffusion of the major elements of the substrate. Moreover, the formation of Kirkendall pores were suppressed in the case of aforementioned coatings. A close-up of the interdiffusion zone for the Ni/Co-modified aluminide coating is shown in Fig. 5. According to the EDS point analyses, it is evident that the strip-like bright precipitates present in the IDZ are rich in Cr (Point 2) compared to the dark gray area of the diffusion coating, which is rich in Al (Point 1). Since the thickness of the outer diffusion coating is larger than the X-ray penetration depth; thus, the XRD results only indicate the presence of β-phase and identification of the phases present in the IDZ cannot be done via this technique. Based on the composition of the substrate, these phases can vary. Fan et al. explained the formation of Cr(W) enriched phases in the IDZ during the phase transformation from γ/γ' microstructure of the superalloy to the β-phase of diffusion coating [51]. It should be noted that the solubility of Cr and W in the dual phase γ/γ' microstructure is higher than that of β-phase [52].

3.3. Hot corrosion behavior

Fig. 6 displays the average thickness of the formed corrosion product layer on the coatings' surface and its phase identification. It is worth noting that the phase composition of the corrosion product revealed by the XRD analysis was similar in all three of the coatings and the only difference was noted on the peak intensities. With this in mind, further characterization was conducted by means of SEM-EDS analysis of the exposed samples.

According to Fig. 6, a considerable improvement in the hot corrosion behavior was observed for the modified coatings, with the NiCo-modified coating exhibiting the best performance. By comparing the XRD patterns before and after the hot corrosion test, it can be noticed that the singular dominant β-phase (Fig. 2c) has been replaced by the γ' phase. Moreover, the diffraction peaks of b phase are still detectable as well as Al_2O_3, indicating the consumption of Al to form the protective alumina layer [24]. In addition, some sulfides and spinels were revealed in the XRD pattern. This could signify the sulfur penetration into the coating; however, it should be studied form microscopic point of view to confirm. It should also be noticed that no peaks corresponding to the oxides of Ni or Co were detected. Although it is possible for these oxides to be formed at the early exposure times; however, they might have been deoxidized by Al (more active) or have been reacted with Al_2O_3, resulting in the formation of $(Ni,Co)(Cr,Al)_2O_4$ [7, 24].

Fig. 7 presents the SEM-EDS analyses of the hot-corroded samples after 100 h. These analyses clearly confirm the hot corrosion performance of the coatings, reported in Fig. 6. As is evident from Fig. 7c, the NiCo-modified coating exhibited the best resistance to the corrosion attack and a large part of the coating remained unaffected, which implies its capability of maintaining and reestablishing the protective alumina scale for prolonged exposure times [24]. In particular, the importance of scale healing is essential during hot corrosion. This is because catastrophic attack will proceed, if the molten salt comes in contact with the underlying depleted substrate, which is unable to reestablish a protective scale [40]. According to the XRD and EDS analyses' results, the corrosion product layer formed on the coatings was primarily consisted of Al_2O_3. This result was expected due to the alumina-forming nature of the diffusion coatings, which arise from their high Al content enabling its selective oxidation [53]. Furthermore, in addition to the sporadic Cr-rich bright precipitates detected within and near the IDZ (Fig. 5), a Cr-rich belt was observed for the NiCo-modified coating after the hot corrosion test (see the inset in Fig. 7c). It is possible that under the high-temperature condition, the Cr atoms have diffused towards the coating surface. Owing to the fact that the γ' phase has partially replaced the β-phase at the sub-surface regions, and considering the high solubility of Cr in the

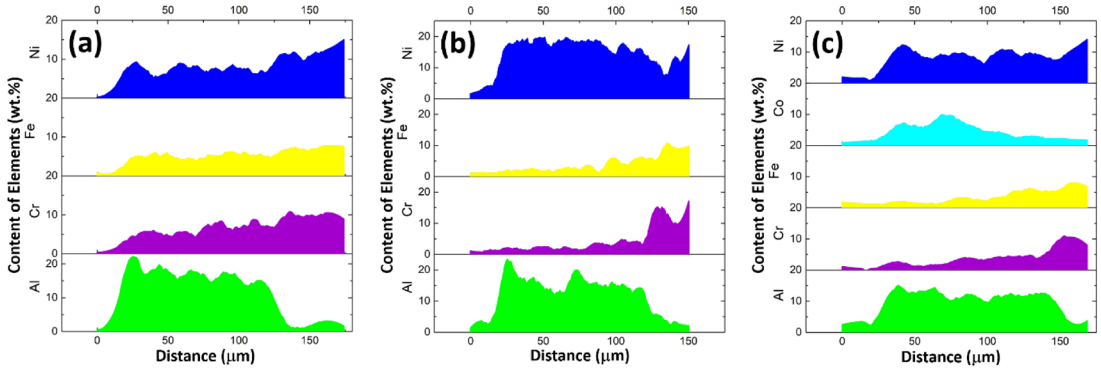

Fig. 4. EDS line scan analyses of the coated samples marked in Fig. 3; (a) simple, (b) Ni-modified, and (c) Ni/Co-modified aluminide coating.

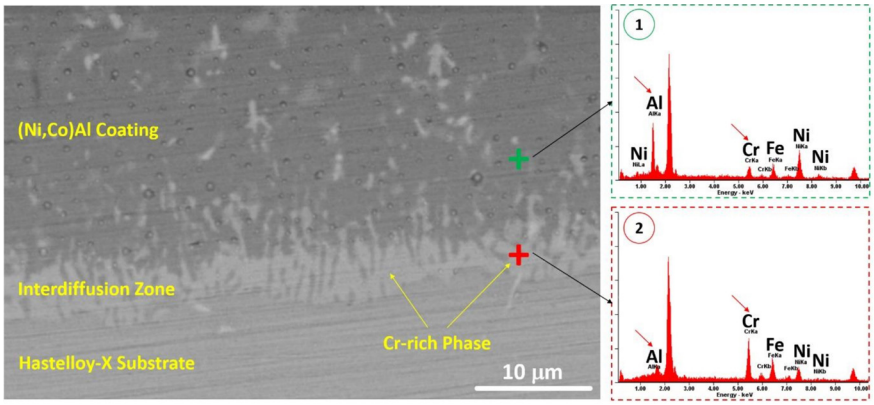

Fig. 5. Cross-section SEM-EDS analyses of the Ni/Co-modified aluminide coating (The arrows point out the peaks' intensities for Al and Cr).

former phase, no distinctive Cr enriched precipitates were found in the upper regions of the coating.

Both the simple aluminide and Ni-modified coatings have considerably suffered from corrosion damage in comparison to the NiCo-modified coating. The prominent mode of accelerated attack below the salt deposit occurs via the penetration of S, which can penetrate into the coating through cracks or voids [54]. It has been reported that S could penetrate as the SO_4^{2-} ions and then interact with alloy elements, especially Cr, to form internal sulfides (reaction 1) [51]. This phenomenon is in accordance with the high tendency of S to combine with Cr, which can be determined by the standard Gibbs free energy changes for the formation of CrS (reaction 2) [55]. Moreover, the consumption of S can accelerate the SO_4^{2-} decomposition (reaction 3), which in turn increases the basicity of the molten salt to a point where it can dissolve Al_2O_3 (reaction 4) [56]. The basic fluxing of Al_2O_3 is reported to be the main degradation mechanism of simple aluminide coatings [36]. Due to the concentration gradient, it is possible for AlO^{2-} to migrate from the salt deposit/oxide scale interface to the salt deposit/air interface, where Al_2O_3 can re-precipitate (reaction 5). However, the newly developed oxides are porous and prone to the transportation of the released O^{2-} back to the salt deposit/oxide scale interface. This process can lead to the increased alkalinity and further fluxing of the Al_2O_3 as a consequence [56]. In this study, a similar scenario was observed for the case of simple aluminide coating (Fig. 7a) and it seems that the discussed self-sustaining process is the reason for this sample's weak corrosion performance.

$$2Cr + 2SO_4^{2-} = 2O^{2-} + 2CrS + 3O_2 \quad (1)$$

$$2Cr + S_2 = 2CrS \ (\Delta G_0 = -405000 + 112.14T) \quad (2)$$

$$SO_4^{2-} = SO_3 + O^{2-} \quad (3)$$

$$Al_2O_3 + O^{2-} = 2AlO^{2-} \quad (4)$$

$$2AlO^{2-} = Al_2O_3 + O^{2-} \quad (5)$$

According to Fig. 7, internal sulfidation is discernible for the simple aluminide and Ni-modified coatings, which indicates a deep penetration of S. On the other hand, the internal sulfidation was significantly

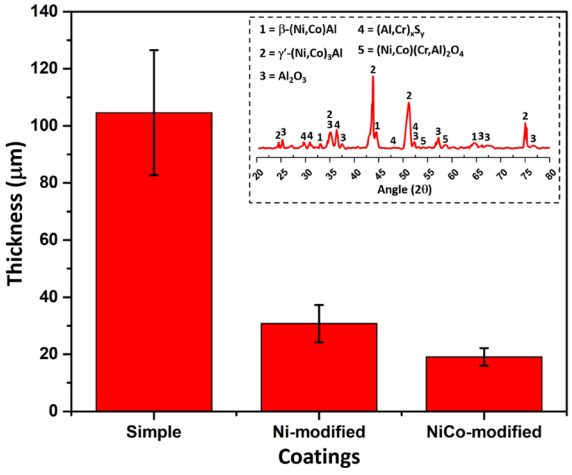

Fig. 6. The measured average thickness of the corrosion product layer for each specimen (the inset shows the XRD results for the NiCo-modified coating after being exposed to Na2SO4 for 100 h).

suppressed in the case of NiCo-modified coating. It is assumed that Co addition to the aluminide coatings can enhance their hot corrosion resistance due to its strong ability to fix S and prevent internal sulfidation [56]. According to the EDS mapping analysis shown in Fig. 7e, a high Co content was still present at the outer regions of the coating and presumably has participated in retarding the S transport. In addition, it has been proposed by Beltran and Shores that the diffusion rate of S in Co is lower than that in Ni by two orders of magnitude [57]. In view of this, the presence of Co in NiAl aluminide coating could alleviate the sulfidation reactions and reduce the internal sulfidation.

4. Conclusions

In this study, Ni/Co-modified aluminide coatings were successfully prepared on the Hastelloy-X superalloy by a combined process of electrodeposition and slurry aluminizing. The following conclusions can

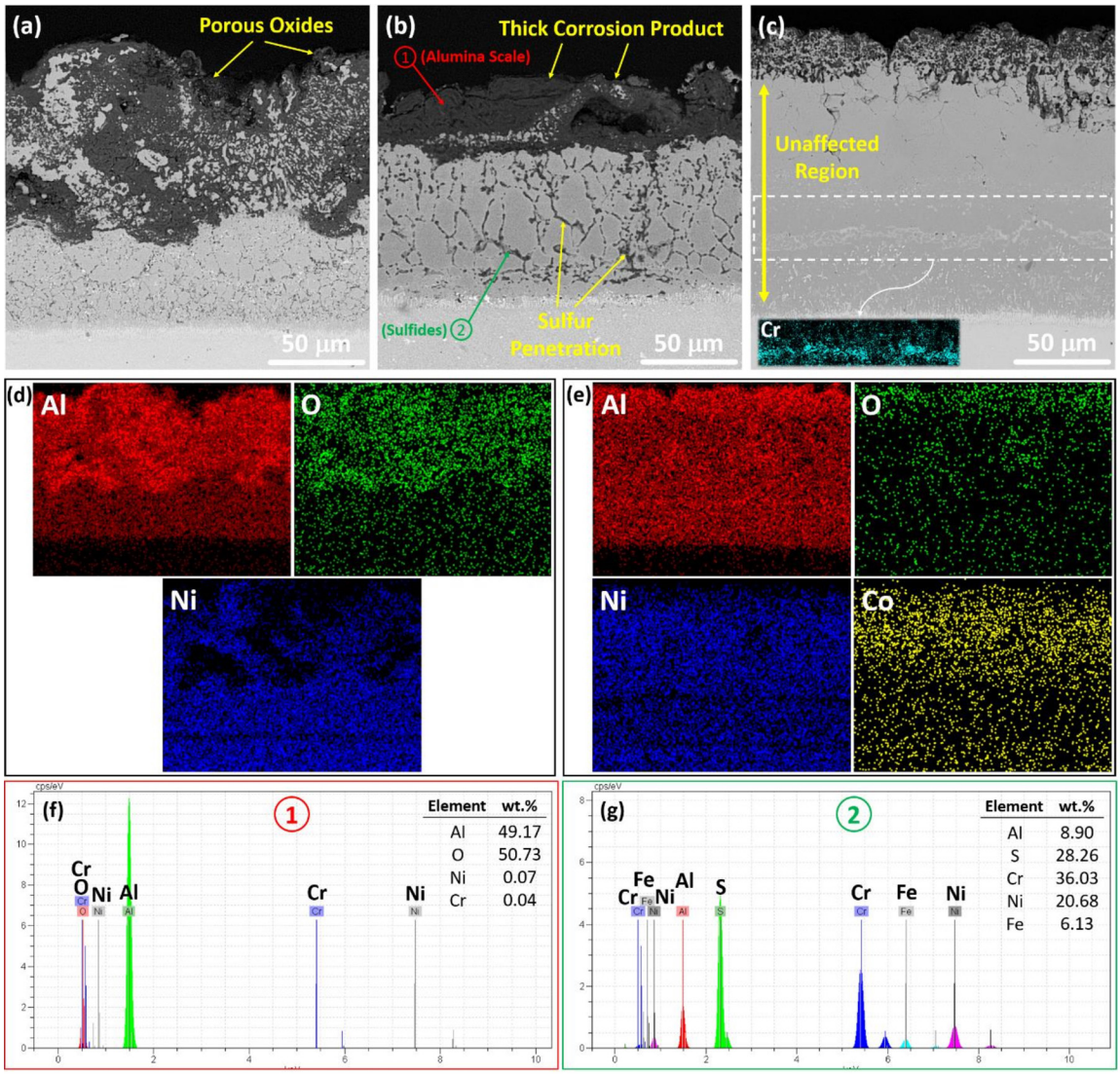

Fig. 7. Cross-section SEM-EDS analyses of the hot-corroded samples; (a) simple aluminide, (b) Ni-modified, (c) NiCo-modified, (d) EDS mapping performed on (a), (e) EDS mapping performed on (c), (f and g) EDS analyses from the marked points in (b).

be drawn from microstructural study and hot corrosion behavior of the obtained coatings:

1. It was established that pre-electrodeposition treatment can be utilized to develop modified slurry aluminide coatings.
2. Both simple and Ni-modified aluminide coatings were composed mainly of thermodynamically stable b-NiAl phase. A singular β-(Ni,Co)Al phase was detected in the case of NiCo-modified coating, in which some of the Ni atoms were replaced by Co. Moreover, some part of Al was remained un-reacted in the case of simple aluminide, which was attributed to the kinetics of aluminization.
3. It was shown that presence of the pre-electrodeposited layers inhibited the outward diffusion flux of elements from the substrate and effectively suppressed the formation of Kirkendall pores.
4. In terms of hot corrosion resistance, the NiCo-modified coating outperformed the other two coatings. This was mainly attributed to the beneficial effect of Co in preventing the internal sulfidation.

Acknowledgments

The authors would like to thank Dr. Mohammad Hossein Allahyarzadeh Bidgoli for his valuable help and advice.

Conflict of interest

The authors declare that there is no conflict of interest.

REFERENCES

[1] T.M. Pollock, S. Tin, Nickel-based superalloys for advanced turbine engines: Chemistry, microstructure, and properties, Journal of Propulsion and Power 22(2) (2006) 361–374.

[2] R.C. Reed, The superalloys: fundamentals and applications, Cambridge university press, England, 2008.

[3] M. Vajdi, F. Sadegh Moghanlou, F. Sharifianjazi, M. Shahedi Asl, M. Shokouhimehr, A review on the Comsol Multiphysics studies of heat transfer in advanced ceramics, Journal of Composites and Compounds 2(2) (2020) 35-43.

[4] M. Alehojat, R. Jafari, P. Karimi, E. Sadeghi, Electron beam-powder bed fusion of Alloy 718: Effect of hot isostatic pressing and thermal spraying on microstructural characteristics and oxidation performance, Surface and Coatings Technology 404 (2020) 126626.

[5] A. Zakeri, E. Bahmani, A. Sabour Rouh Aghdam, B. Saeedi, M. Bai, A study on the effect of nano-CeO_2 dispersion on the characteristics of thermally-grown oxide (TGO) formed on NiCoCrAlY powders and coatings during isothermal oxidation, Journal of Alloys and Compounds 835 (2020) 155319.

[6]M. Bai, Fabrication and Characterization of Thermal Barrier Coatings, PhD thesis, University of Manchester, 2015.

[7] A. Zakeri, E. Bahmani, A.S.R. Aghdam, Impact of MCrAlY feedstock pow-

der modification by high-energy ball milling on the microstructure and high-temperature oxidation performance of HVOF-sprayed coatings, Surface and Coatings Technology 395 (2020) 125935.
[8] A. Zakeri, E. Bahmani, A. Sabour Rouh Aghdam, B. Saeedi, A comparative study on the microstructure evolution of conventional and nanostructured MCrAlY powders at high-temperature, Surface and Coatings Technology 389 (2020) 125629.
[9] A. Zakeri, F. Ghadami, A. Sabour Rouhaghdam, B. Saeedi, Study on production of modified MCrAlY powder with nano oxide dispersoids as HVOF thermal spray feedstock using mechanical milling, Materials Research Express 7 (2019) 015030.
[10] M. Masoumi Balashadehi, P. Nourpour, A. Sabour Rouh Aghdam, M.H. Allahyarzadeh, A. Heydarzadeh, M. Hamdi, The formation, microstructure and hot corrosion behaviour of slurry aluminide coating modified by Ni/Ni-Co electrodeposited layer on Ni-base superalloy, Surface and Coatings Technology 402 (2020) 126283.
[11] F. Ghadami, A. Zakeri, A.S.R. Aghdam, R. Tahmasebi, Structural characteristics and high-temperature oxidation behavior of HVOF sprayed nano-CeO_2 reinforced NiCoCrAlY nanocomposite coatings, Surface and Coatings Technology 373 (2019) 7–16.
[12] F. Ghadami, A. Sabour Rouh Aghdam, A. Zakeri, B. Saeedi, P. Tahvili, Synergistic effect of CeO_2 and Al_2O_3 nanoparticle dispersion on the oxidation behavior of MCrAlY coatings deposited by HVOF, Ceramics International 46(4) (2020) 4556–4567.
[13] M. Bai, L. Reddy, T. Hussain, Experimental and thermodynamic investigations on the chlorine-induced corrosion of HVOF thermal sprayed NiAl coatings and 304 stainless steels at 700 °C, Corrosion Science 135 (2018) 147–157.
[14] M. Bai, B. Song, L. Reddy, T. Hussain, Preparation of MCrAlY–Al_2O_3 Composite Coatings with Enhanced Oxidation Resistance through a Novel Powder Manufacturing Process, Journal of Thermal Spray Technology 28(3) (2019) 433–443.
[15] H. Chi, M.A. Pans, M. Bai, C. Sun, T. Hussain, W. Sun, Y. Yao, J. Lyu, H. Liu, Experimental investigations on the chlorine-induced corrosion of HVOF thermal sprayed Stellite-6 and NiAl coatings with fluidised bed biomass/anthracite combustion systems, Fuel 288 (2021) 119607.
[16] A. Abuchenari, H. Ghazanfari, M. Siavashi, M. Sabetzadeh, S. Talebi, Z. Karami Chemeh, A. Jamavari, A review on development and application of self-healing thermal barrier composite coatings, Journal of Composites and Compounds 2(3) (2020) 147–154
[17] A. Firouzi, K. Shirvani, The structure and high temperature corrosion performance of medium-thickness aluminide coatings on nickel-based superalloy GTD111, Corrosion Science 52(11) (2010) 3579–3585.
[18] M.C. Galetz, X. Montero, M. Mollard, M. Günthner, F. Pedraza, M. Schütze, The role of combustion synthesis in the formation of slurry aluminization, Intermetallics 44 (2014) 8–17.
[19] Z.D. Xiang, J.S. Burnell-Gray, P.K. Datta, Aluminide coating formation on nickel-base superalloys by pack cementation process, Journal of Materials Science 36(23) (2001) 5673–5682.
[20] Y. Wang, J. Wang, H. Hu, J. Meng, X. Zhao, Effect of Y_2O_3 content in the pack mixtures on the cyclic-oxidation of Y_2O_3-modified low temperature aluminide coatings on 309 stainless steel, Vacuum 158 (2018) 101-112.
[21] G.W. Goward, Progress in coatings for gas turbine airfoils, Surface and Coatings Technology 108–109 (1998) 73–79.
[22] T. Kepa, F. Pedraza, F. Rouillard, Intermetallic formation of Al-Fe and Al-Ni phases by ultrafast slurry aluminization (flash aluminizing), Surface and Coatings Technology 397 (2020) 126011.
[23] J.T. Bauer, X. Montero, M.C. Galetz, Fast heat treatment methods for al slurry diffusion coatings on alloy 800 prepared in air, Surface and Coatings Technology 381 (2020) 125140.
[24] Q.X. Fan, S.M. Jiang, H.J. Yu, J. Gong, C. Sun, Microstructure and hot corrosion behaviors of two co modified aluminide coatings on a ni-based superalloy at 700 c, Applied Surface Science 311 (2014) 214–223.
[25] M. Zagula-Yavorska, J. Morgiel, J. Romanowska, J. Sieniawski, TEM analysis of the hafnium-doped aluminide coating deposited on Inconel 100 superalloy, Vacuum 116 (2015) 115–120.
[26] M. Zagula-Yavorska, J. Morgiel, J. Romanowska, J. Sieniawski, Nanoparticles in zirconium-doped aluminide coatings, Materials Letters 139 (2015) 50–54.
[27] W. Ren, C. Xiao, Q. Li, J. Song, L. He, C. Cao, Microstructure evolution of cobalt aluminide coating on nickel-based superalloys during exposure at 1050 °c, Vacuum 106 (2014) 39–45.
[28] S.A. Azarmehr, K. Shirvani, A. Solimani, M. Schutze, M.C. Galetz, Effects of Pt and Si on the low temperature hot corrosion of aluminide coatings exposed to Na_2SO_4 60 mol% V_2O_5 salt, Surface and Coatings Technology 362 (2019) 252–261.
[29] Y. Zhou, X. Zhao, C. Zhao, W. Hao, X. Wang, P. Xiao, The oxidation performance for Zr-doped nickel aluminide coating by composite electrodepositing and pack cementation, Corrosion Science 123 (2017) 103–115.
[30] Y. Wang, Y. Zhang, G. Liang, Q. Ding, Low temperature formation of aluminide coatings on the electrodeposited nanocrystalline Ni and its oxidation resistance with La2O3/CeO2 nanoparticle dispersion, Vacuum 173 (2020) 109148.
[31] Y.B. Zhou, H.T. Hu, H.J. Zhang, Oxidation behavior of aluminide coatings on carbon steel with and without electrodeposited Ni-CeO_2 film by low-temperature pack cementation, Vacuum 86 (2) (2011) 210–217.
[32] M.H. Allahyarzadeh, M. Aliofkhazraei, A.S. Rouhaghdam, ELectrodeposition on superalloy substrates: A review, Surface Review and Letters 23 (2016) 1630001.
[33] A. Karimzadeh, A.S. Rouhaghdam, Effect of Nickel Pre-Plated on Microstructure and Oxidation Behavior of Aluminized AISI 316 Stainless Steel, Materials and Manufacturing Processes 31 (1) (2016) 87–94.
[34] M. Safari, F. Shahriari Nogorani, Formation mechanism of high activity aluminide coating on Ni-CeO_2 coated Rene 80 alloy, Surface and Coatings Technology 329 (2017) 218–223.
[35] M. Qiao, C. Zhou, Codeposition of Co-Al-Y on nickel base superalloys by pack cementation process, Corrosion Science 75 (2013) 454–460.
[36] M. Qiao, C. Zhou, Hot corrosion behavior of Co modified NiAl coating on nickel base superalloys, Corrosion Science 63 (2012) 239–245.
[37] S. Mahini, S. Khameneh Asl, T. Rabizadeh, H. Aghajani, Effects of the pack Al content on the microstructure and hot corrosion behavior of aluminide coatings applied on Inconel-600, Surface and Coatings Technology 397 (2020) 125949.
[38] D. He, H. Guan, X. Sun, X. Jiang, Manufacturing, structure and high temperature corrosion of palladium-modified aluminide coatings on nickel-base superalloy M38, Thin Solid Films 376 (2000) 144–151.
[39] M. Salehi Doolabi, B. Ghasemi, S.K. Sadrnezhaad, A. Habibollahzadeh, K. Jafarzadeh, Hot corrosion behavior and near-surface microstructure of a "low-temperature high-activity Cr-aluminide" coating on inconel 738LC exposed to Na-2SO_4, Na_2SO_4 + V_2O_5 and Na_2SO_4 + V_2O_5 + NaCl at 900 °C, Corrosion Science 128 (2017) 42–53.
[40] M.N. Task, B. Gleeson, F.S. Pettit, G.H. Meier, Compositional effects on the Type I hot corrosion of B-NiAl alloys, Surface and Coatings Technology 206(7) (2011) 1552–1557.
[41] C.A. Schneider, W.S. Rasband, K.W. Eliceiri, NIH Image to ImageJ: 25 years of image analysis, Nature Methods 9(7) (2012) 671–675.
[42] R. Jafari, E. Sadeghi, High-temperature corrosion performance of HVAF-sprayed NiCr, NiAl, and NiCrAlY coatings with alkali sulfate/chloride exposed to ambient air, Corrosion Science 160 (2019) 108066.
[43] P.D.F. ICDD, International Centre for Diffraction Data, Microscopy Today 21(S1) (2013) 8–8.
[44] A. Brenner, Electrodeposition of alloys: principles and practice, First Ed., Elsevier, Netherlands, 1963.
[45] M. Ferdosi Heragh, S. Eskandarinezhad, A. Dehghan, Ni-Cu matrix composite reinforced with CNTs: preparation, characterization, wear and corrosion behavior, inhibitory effects, Journal of Composites and Compounds 2(3) (2020) 123–128.
[46] E. Bahmani, A. Zakeri, A. Sabour Rouh Aghdam, A fast and efficient approach to fabricate tarnish-resistant nanocrystalline Ag-Ge thin films by direct current electrodeposition, Materials Letters 274 (2020) 127991.
[47] E. Bahmani, A. Zakeri, A. Sabour Rouh Aghdam, Microstructural analysis and surface studies on Ag-Ge alloy coatings prepared by electrodeposition technique, Journal of Materials Science 56(10) (2021) 6427-6447.
[48] A. Karimzadeh, A.S. Rouhaghdam, M. Aliofkhazraei, R. Miresmaeili, Sliding wear behavior of Ni–Co–P multilayer coatings electrodeposited by pulse reverse method, Tribology International 141 (2020) 105914.
[49] A. Karimzadeh, M. Aliofkhazraei, F.C. Walsh, A review of electrodeposited Ni-Co alloy and composite coatings: Microstructure, properties and applications, Surface and Coatings Technology 372 (2019) 463–498.
[50] M.S. Safavi, M. Tanhaei, M.F. Ahmadipour, R.G. Adli, S. Mahdavi, F.C. Walsh, Electrodeposited Ni-Co alloy-particle composite coatings: a comprehensive review, Surface and Coatings Technology 382 (2020) 125153.
[51] R.D. Liu, S.M. Jiang, H.J. Yu, J. Gong, C. Sun, Preparation and hot corrosion behaviour of Pt modified AlSiy coating on a Ni-based superalloy, Corrosion Science 104 (2016) 162–172.
[52] C.C. Jia, K. Ishida, T. Nishizawa, Partition of alloying elements between γ (A1), γ' (L12), and β (B2) phases in Ni-Al base systems, Metallurgical and Materials Transactions A 25(3) (1994) 473-485.
[53] T.J. Nijdam, L.P.H. Jeurgens, W.G. Sloof, Promoting exclusive α-Al_2O_3

growth upon high-temperature oxidation of NiCrAl alloys: experiment versus model predictions, Acta Materialia 53(6) (2005) 1643-1653.
[54] M. Bai, H. Jiang, Y. Chen, Y. Chen, C. Grovenor, X. Zhao, P. Xiao, Migration of sulphur in thermal barrier coatings during heat treatment, Materials & Design 97 (2016) 364–371.
[55] C.Y. Jiang, Y.F. Yang, Z.Y. Zhang, Z.B. Bao, M.H. Chen, S.L. Zhu, F.H. Wang, A Zr-doped single-phase Pt-modified aluminide coating and the enhanced hot corrosion resistance, Corrosion Science 133 (2018) 406–416.
[56] Q.X. Fan, S.M. Jiang, D.L. Wu, J. Gong, C. Sun, Preparation and hot corrosion behaviour of two Co modified NiAl coatings on a Ni-based superalloy, Corrosion Science 76 (2013) 373–381.
[57] A.M. Beltran, D.A. Shores, Hot Corrosion, The Superalloys, CT Sims and WC Hagel, Wiley, New York 1972.